CIVIL ENGINEERING JOURNAL

Article no. 39

THE CIVIL ENGINEERING JOURNAL 4-2025

FLEXURAL PERFORMANCE OF CONCRETE T-BEAMS REINFORCED WITH UHPC: EXPERIMENTAL AND THEORETICAL ANALYSIS

Xilong Chen[1], Guangqing Xiao[1], Fucheng Wu[1], Mingtao Ye[2], and Shaohua He[2]

1. *Guangzhou Guangjian Construction Engineering Testing Center Co., Ltd, No. 295 Baiyunda Road, Baiyun District, Guangzhou, China*
2. *Guangdong University of Technology, School of Civil and Transportation Engineering, No.100 Waihuangxi Road, Panyu District, Guangzhou, China; hesh@gdut.edu.cn*

Received: *03.02.2025*
Received in revised form: *11.09.2025*
Accepted: *02.12.2025*

ABSTRACT

The use of ultra-high performance concrete (UHPC) for strengthening deficient reinforced concrete T-beam bridges has gained popularity in recent years. Despite its growing application, the failure mechanisms of UHPC-reinforced T-beams under flexural loads, along with corresponding design methods, require further exploration. This study aims to investigate the flexural performance of T-beams enhanced with thin UHPC layers through a combination of theoretical analysis and experimental testing. An analytical model is proposed to estimate the cracking and ultimate resistances of UHPC-strengthened T-beams subjected to bending moments. To validate this model, three concrete T-beam specimens with varying UHPC thicknesses were fabricated and tested to failure. The observed failure modes, load-displacement responses, and strain distributions of the T-beams are presented and analyzed. Results indicate that the incorporation of UHPC layers markedly improves the flexural performance of the T-beams: increasing the layer thickness from 0 mm to 50 mm resulted in a 167.8% enhancement in flexural stiffness, a 241.0% increase in initial cracking load, and a 40.8% rise in ultimate flexural capacity. The relative error between predictions from the developed model and experimental outcomes was found to be less than 10%, underscoring the model's validity and indicating sufficient safety margins. These findings offer significant insights for the design of flexural strengthening techniques employing thin UHPC layers in defective concrete T-beams, contributing to enhanced structural integrity and longevity.

KEYWORDS

Concrete T-beam, UHPC, Strengthening, Flexural performance, Predictive model

INTRODUCTION

The increasing operational demands on transportation infrastructure and the accelerated deterioration of aging concrete bridges have made structural reinforcement a critical focus in civil engineering [1-3]. Conventional strengthening techniques, including section enlargement with

normal concrete (NC), bonded steel sheets, and external prestressing [4, 5], have been extensively adopted to improve load-bearing capacity and durability of the existing bridges. However, these methods are frequently associated with limitations such as increased structural self-weight, susceptibility to corrosion, and localized stress concentrations at anchorage regions [6]. These challenges necessitate the development of advanced materials that integrate structural efficiency with sustainable performance.

Ultra-high-performance concrete (UHPC), characterized by its exceptional compressive strength (>150 MPa), strain-hardening tensile properties, and superior durability, has emerged as a transformative material in deficient bridge rehabilitation [7]. International engineering applications have demonstrated its potential. For instance, a 30 mm UHPC overlay applied to the Rhine Bridge in Switzerland enhanced impact resistance by approximately 60% [8], while the U.S. Route 46 Bridge project achieved a 30% reduction in construction time through UHPC's rapid curing properties [9]. In China, the rehabilitation of the Wenzaobang Bridge using UHPC effectively reduced mid-span deflection by 42% by mitigating carbonation-induced cracking in T-beams [10]. These cases highlight UHPC's ability to overcome the limitations of traditional reinforcement methods.

The mechanical benefits of UHPC reinforcing techology have been further validated through experimental investigations. Yin et al. [11] reported that UHPC overlays in the tensile zones of T-beams changed failure modes of the structure from brittle shear to ductile flexure, with crack density increasing proportionally to overlay thickness. Men et al. [12] expanded on these findings, demonstrating that extended UHPC reinforcement lengths optimized tensile utilization, allowing reinforced beams to achieve 95% of theoretical ultimate bending resistance. These studies collectively confirm UHPC's role in enhancing both load capacity and ductility in deteriorated structural memebers.

Despite these advancements, critical knowledge gaps remain regarding the flexural behavior of UHPC-strengthened concrete T-beams, particularly concerning the influence of UHPC layer thickness on stiffness evolution, strain compatibility, and the mechanisms of composite interaction. To address these issues, a predictive model for flexural capacity was developed based on the conversion section method in accordance with Chinese design codes [13]. Three strengthened concrete T-beams with UHPC layer thicknesses of 0 mm, 30 mm, and 50 mm were designed and tested under four-point loading conditions, with systematic analyses of failure modes, load-deflection curves, and strain distribution characteristics. The accuracy of the proposed model was subsequently validated against experimental results, providing both theoretical insights and practical guidance for optimizing UHPC-enhanced strengthening strategies in bridge rehabilitations.

PREDICTION OF FLEXURAL STRENGTH OF UHPC-REINFORCED T-BEAMS

Basic Assumptions

Based on the existing conversion section method for calculating the flexural capacity of UHPC-strengthened concrete T-beams, the flexural capacity of a UHPC-strengthened reinforced concrete (RC) T-beam primarily depends on four components: the tensile reinforcement in the original beam, the high-strength steel mesh or reinforcement bars within the UHPC layer, the concrete in the compressive zone, and the tensile strength of the UHPC. This section adopts the transformed section method for analysis, based on existing literature and design codes [13, 14]. The following fundamental assumptions are made for calculating the flexural capacity:

(1) During flexural loading of a UHPC-strengthened RC T-beam, the strain distribution along the depth of the NC and UHPC sections always satisfies the plane section assumption;

(2) No relative slip occurs at the interface between the UHPC strengthening layer and the existing RC T-beam;
(3) After cracking, the original concrete is considered no longer effective in carrying tensile stress. The strain hardening behavior of reinforcement and the contribution of compressive reinforcement in the flange of the original beam are neglected. Tensile force is entirely resisted by the tensile reinforcement in the original beam and the steel mesh or reinforcement bars in the UHPC layer;
(4) The influence of bond-slip between reinforcement and concrete, self-weight of the beam, as well as shrinkage and creep of the UHPC layer and the original concrete, are neglected;
(5) The strain hardening behavior of UHPC material after tensile cracking is taken into account.

Material Constitutive Model

In the calculation and analysis of the ultimate flexural capacity of UHPC-strengthened beams, the constitutive relationships of NC, steel reinforcement, and UHPC were selected in accordance with the Chinese design code [15]. The stress-strain curve of the steel reinforcement includes a yield plateau, while the UHPC material does not cease to bear load immediately after cracking. This is primarily attributed to the bridging effect of steel fibers, resulting in mechanical behavior that significantly differs from that of conventional concrete. The constitutive models of the three materials are shown in Figure 1.

The equation for the compressive constitutive model of NC is:

$$\sigma_N^c = \begin{cases} f_{cu}[1-(1-\frac{\varepsilon_N^c}{\varepsilon_0})^2], \varepsilon_N^c \le \varepsilon_0 \\ f_c, \varepsilon_0 < \varepsilon_N^c \le \varepsilon_{cu} \end{cases} \quad (2.1)$$

The equation for the tension constitutive model of steel reinforcement is:

$$\sigma_s = \begin{cases} E_s\varepsilon_s, 0 \le \varepsilon_s \le \varepsilon_y \\ f_y, \varepsilon_y < \varepsilon_s \le \varepsilon_u \end{cases} \quad (2.2)$$

The equation for the tension constitutive model of UHPC is:

$$\sigma_u^t = \begin{cases} E_c\varepsilon_u^t, 0 < \varepsilon_u^t \le \varepsilon_{tu} \\ f_{tu}, \varepsilon_{tu} < \varepsilon_u^t \le \varepsilon_{tp} \end{cases} \quad (2.3)$$

Where, f_{cu}-The axial compressive strength of concrete; ε_0-The concrete compressive strain corresponding to the stress f_{cu}, taken as 0.0015; ε_{cu}-The ultimate compressive strain of concrete, taken as 0.002; E_s-The elastic modulus of steel reinforcement; f_y-The yield stress of steel reinforcement; ε_y-The tensile strain of steel reinforcement corresponding to the stress f_y, taken as 0.002; ε_u-The ultimate tensile strain of steel reinforcement, taken as 0.075; E_c-The elastic modulus of UHPC; f_{tu}-The peak tensile stress of UHPC; ε_{tu}-The peak tensile strain of UHPC, taken as 0.001; ε_{tp}-The ultimate strain of UHPC, taken as 0.002.

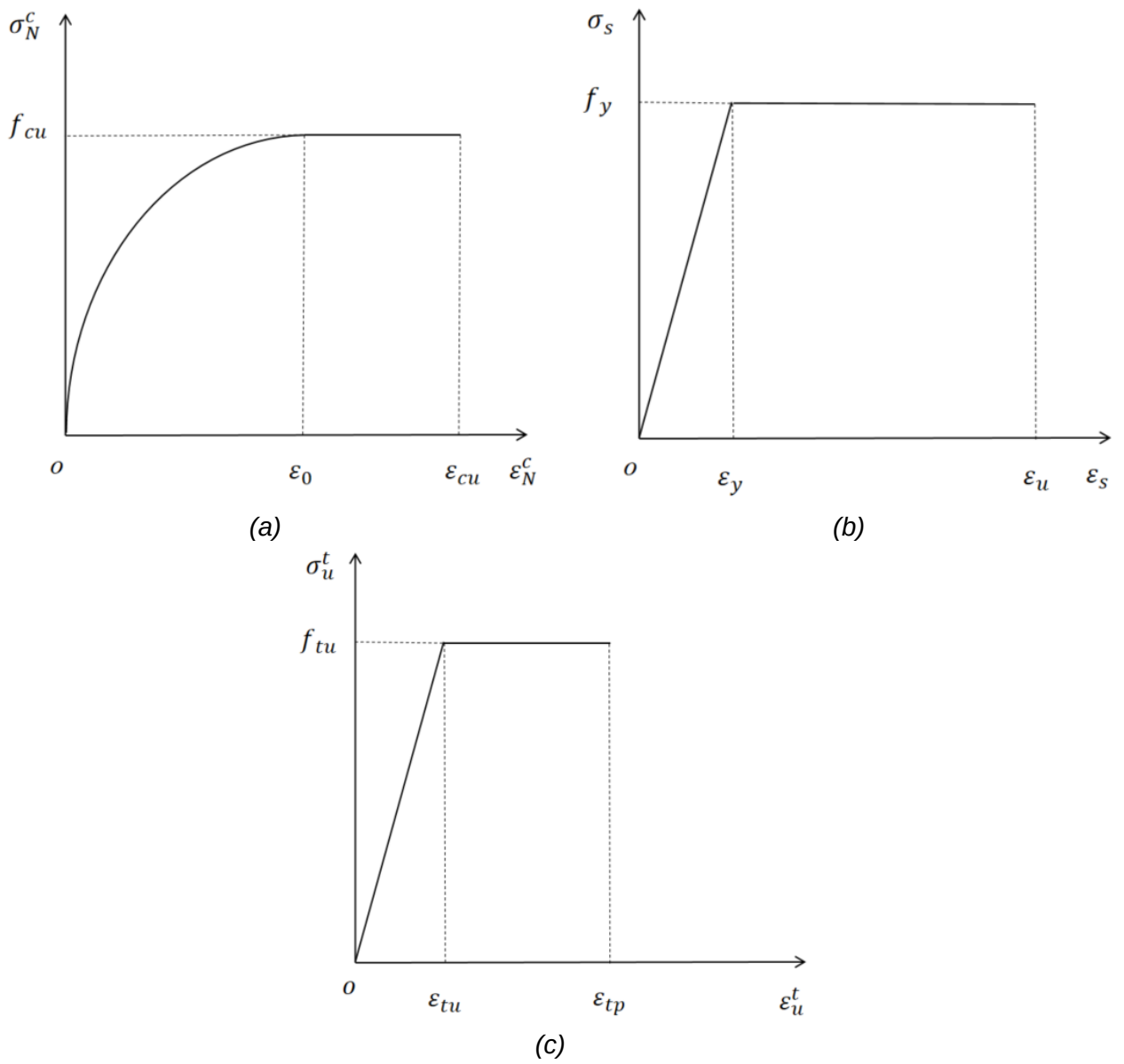

Fig. 1 - Constitutive models of the three materials: (a) NC compression; (b) Steel tension (c) UHPC tension

Analytical Formulation Proposed

The fundamental principle of the conversion section method involves combining the original T-beam with a layer of UHPC to create a new, effective section. In this analysis, the mechanical properties of the UHPC layer are translated into an equivalent NC section. The modulus conversion factor, denoted as n, is defined as the ratio of the modulus of elasticity of the UHPC (E_{uhpc}) to that of NC (E_c). This can be expressed as $n = E_{uhpc}/E_c$. Once the new effective section is established, the flexural capacity can be calculated based on the assumption of plane sections. Figure 2 shows the schematic cross-sectional diagrams and stress-strain distribution diagrams of the UHPC strengthened T-beam.

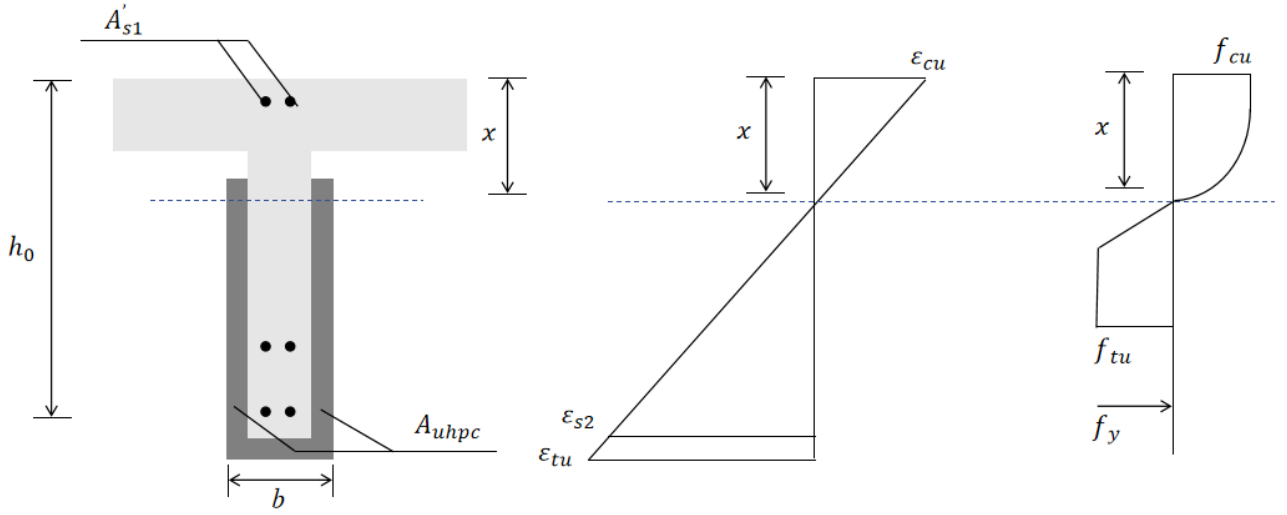

Fig. 2 - Stress-strain distribution across the cross-section of the T-beam specimens

According to the code [13], when flexural strengthening is applied to the tension zone of a T-beam, the flexural load-bearing capacity of the positive section should be calculated using the following formula:

$$M_d = f_{cd1}bx(h_0 - \frac{x}{2}) + f_{sd1}^{'}A_{s1}^{'}(h_0 - a_{s1}^{'}) \tag{2.4}$$

The height of the concrete compression zone can be calculated using the following formula:

$$f_{cd1}bx = f_{sd1}A_{s1} - f_{sd1}^{'}A_{s1}^{'} + \sigma_{s2}A_{s2} \tag{2.5}$$

$$\sigma_{s2} = \varepsilon_{s2}E_{s2} \le f_{sd2} \tag{2.6}$$

The height of the concrete compression zone should also meet the following conditions:

$$2a_{s1}^{'} \le x \le \xi_b h_{01} \tag{2.7}$$

Where, M_d-Design moment; f_{cd1}-Design value of axial compressive strength of original concrete components; f_{sd1}, $f_{\mathrm{sd1}}^{'}$-Design strengths for tensile and compressive, respectively of longitudinal steel bars in the original component; $A_{S1}, A_{S1}^{'}$-The cross-sectional area of longitudinal ordinary steel bars in the tensile and compressive zones, respectively, of the original component; $a_{s1}^{'}$-The distance from the longitudinal ordinary reinforcement in the compression zone to the extreme compression fiber of the section; A_{s2}-Add cross-sectional area of ordinary steel rebars; b-Section width of reinforced components; h_{01}-Effective height of original section; h_0-Effective height of reinforced section; x-Height of concrete compression zone; σ_{s2}-Add tensile stress to longitudinal steel rebars; E_{s2}-Add elastic modulus of longitudinal ordinary steel bars; ε_{s2}-Add tensile strain of longitudinal steel rebars; f_{sd2}-Design value of tensile strength for newly added longitudinal steel rebars; ξ_b-Height of the compression zone at the relative boundary of the normal section.

For T-beams strengthened with a UHPC layer in the tensile zone, the cracking load under flexural loading should be calculated using the following formula:

$$M_{cr} = f_{cd1}b(h_0 - x)(\frac{h_0 - x}{8}) + \frac{1}{8}f_{sd1}^{'}A_{s1}^{'}(h_0 - x) + \frac{6}{7}\beta A_{uhpc}f_{uhpc}(h_0 - 0.8x) \tag{2.8}$$

For T-beams strengthened with a UHPC layer in the tensile zone, the bending capacity of the cross-section under bending rebars should be calculated according to the following formula:

$$M_u = f_{cd1}bx(h_0 - \frac{x}{2}) + f_{sd1}^{'}A_{s1}^{'}(h_0 - a_{s1}^{'}) + \beta A_{uhpc}f_{uhpc}(h_0 - 0.8x) \tag{2.9}$$

Where, A_{uhpc}-Cross-sectional area of UHPC layer; f_{uhpc}-Tensile strength of UHPC; h_0-Effective height of UHPC reinforced section; β-Transfer effect coefficient, taken as 0.07. Other symbols have the same meaning as the formula (2.4).

EXPERIMENTAL PROGRAM

Specimen Design and Preparations

Figure 3 shows the configuration and geometric dimensions of the T-beams, which have a length of 3,000 mm, a height of 520 mm, and a width of 640 mm. The web has a width of 120 mm and a height of 440 mm. The internal longitudinal reinforcement consists of 10 mm (Φ10) and 16 mm (Φ16) diameter steel rebars. The UHPC layer covers the entire web on both sides and the bottom of the T-beam. The interface between the UHPC and NC was enhanced by short steel rebars implanted after surface roughening treatment.

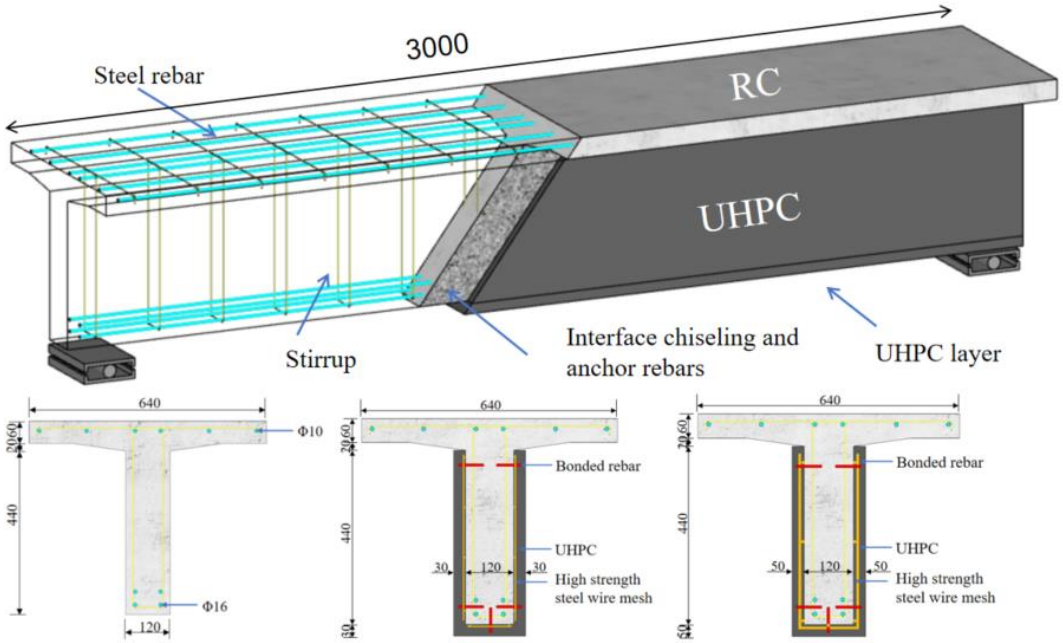

Fig. 3 - Configuration of UHPC-reinforced T-beam specimens

Table 1 provides details of the test T-beam specimens. A total of three T-beams were designed and fabricated, with UHPC layer thicknesses of 30 mm and 50 mm, respectively. Steel wire mesh and steel rebars were embedded within the UHPC layers. The T-beams are labeled as follows: "RC-TH0" refers to the unreinforced concrete T-beam, "UN-TH30" indicates the T-beam reinforced with a 30 mm-thick UHPC layer, and "UN-TH50" denotes the T-beam reinforced with a 50 mm-thick UHPC layer.

Tab. 1 - Information of UHPC reinforced T-beams

Specimen code	Reinforcing form	UHPC thickness	Reinforcement ratio	Interface treatment
RC-TH0	--	--	1.24%	--
UN-TH30	UHPC layer	30 mm		Chiseling + shear steel rebars
UN-TH50		50 mm		

Figure 4 shows the main process of T-beam specimen construction: (a) Fabricating the mold and steel rebars framework; (b) Pouring NC and curing for 28 days; (c) Surface roughening of the NC and embedding the steel rebars; (d) Pouring UHPC and curing for 28 days.

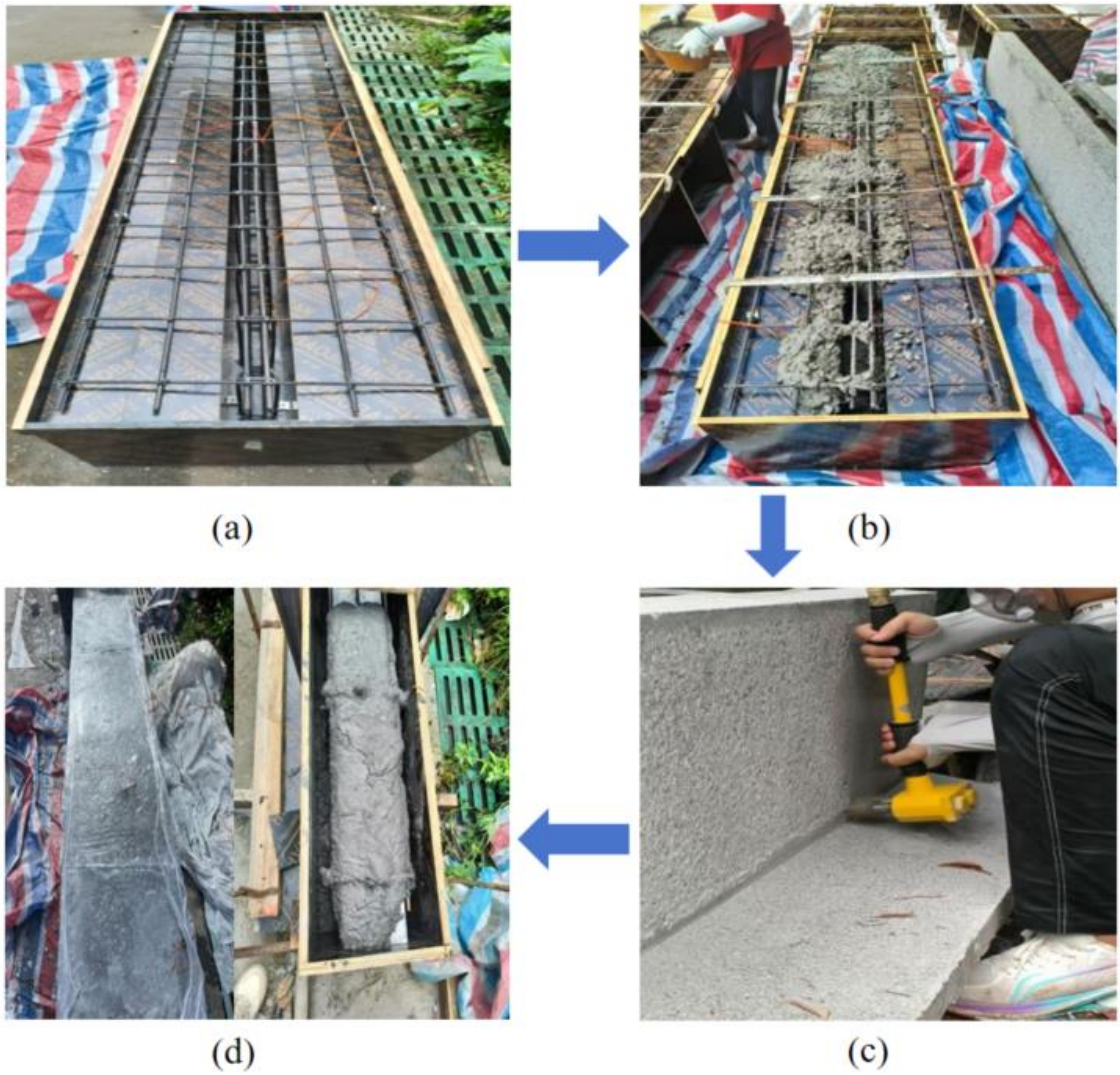

Fig. 4 - Fabrication of test beam specimens

Material Properties

The NC used in this experiment was C55 grade concrete with a target compressive strength of 55 MPa, while the UHPC used is a commercial pre-mixed dry material, with a steel fiber content of 2% and a target compressive strength of 120 MPa. The material properties of NC and UHPC were determined based on Chinese codes [15, 16]. The measured compressive strength and elastic modulus of UHPC cubes were 136.5 MPa and 46.7 GPa, respectively, while the compressive strength and elastic modulus of NC were 59.1 MPa and 36.1 GPa, respectively. The internal steel rebars used HRB400, with measured yield strength, ultimate tensile strength, and elastic modulus of 483 MPa, 594 MPa, and 200 GPa, respectively.

Test Step and Instrumentation

Figure 5(a) shows the loading schematic of the specimens. A 10,000-kN servo press was used to apply the load, with a distribution beam achieving a four-point bending load. The test

T-beams were installed on fixed-hinged supports and sliding-hinged supports. The loading procedure was divided into two steps: (i) Preloading stage: A load of 10 kN was applied to eliminate initial defects in the loading system and to check the operational status of the equipment. (ii) Formal loading stage: A monotonic incremental method was used, with an initial load increase of 50 kN per step, holding for 1 minute at each step. When cracks larger than 0.1 mm first appeared in the beam specimen, the loading was switched to displacement control (1 mm/min) until the T-beam failed.

During the testing process, the primary measured parameters included the deflection at various points of the beam, concrete strain, steel reinforcement strain, and interfacial slip between the UHPC and NC layers. Figure 5(b) shows the layout of strain gauges and displacement transducers on the test beam. The deflection data were obtained using vertically mounted LVDT displacement transducers, which were positioned at the L/4, mid-span, and 3L/4 sections along the bottom of the beam. Concrete and reinforcement strains were measured with electrical resistance strain gauges and collected via a strain acquisition system. At the mid-span section, multiple strain measurement points were arranged at the top and bottom surfaces of the concrete. To quantify the relative slip at the UHPC-NC interface, a horizontal displacement transducer was mounted on the UHPC surface at the right end of the beam, with an angle steel fixture installed on the NC.

Figures 5(c) and (d) show the test acquisition instruments used during the experiment. The load was measured by a pressure sensor connected to the test acquisition system. During the load-holding phases, crack widths were observed and crack propagation was recorded. Under each load level, the widths of multiple cracks were measured individually. The maximum crack width observed during the measurement process was defined as the representative crack width for that specific load level.

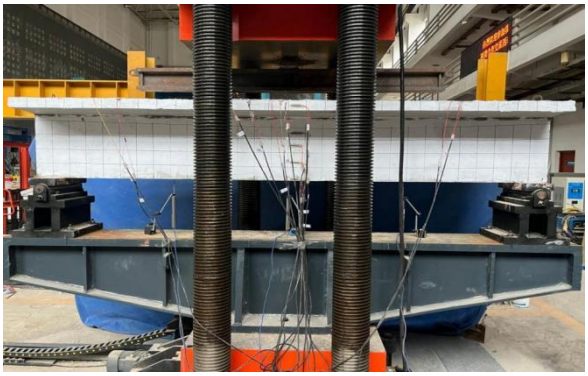

(a)

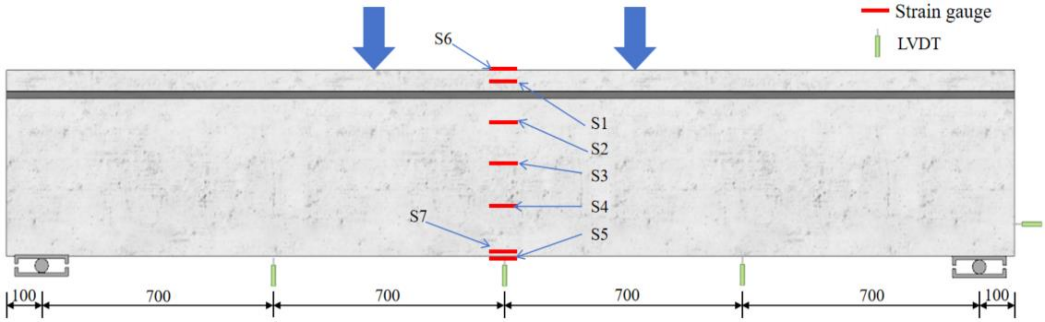

(b)

(c)

(d)

Fig 5 - Loading and strain gauge layout: (a) Loading diagram; (b) Strain gauge layout; (c) Test acquisition instrument; (d) Crack comprehensive tester.

Failure Pattern

Figure 6 illustrates the failure patterns observed in the tested T-beams. For the RC-TH0 specimen, cracks initially formed at the bottom of the T-beam and gradually extended along the sides to the top flange. As the tensile reinforcement bars at the bottom yielded, multiple cracks rapidly propagated, leading to an increase in the downward deflection of the beam, ultimately causing the concrete compression zone beneath the top loading point to collapse. In contrast, the beams reinforced with UHPC layers (e.g., UN-TH30 & UN-TH50) exhibited more concentrated cracking patterns. At the point of failure, the width of a primary crack increased rapidly while the widths of the other cracks widened to a lesser extent. This behavior suggests that the steel fibers in the UHPC provided a practical bridging effect, which helped to suppress both the formation and development of cracks during the failure process.

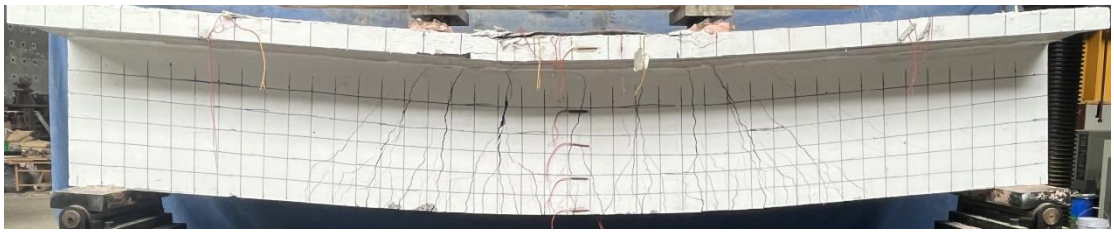

(a)

(b)

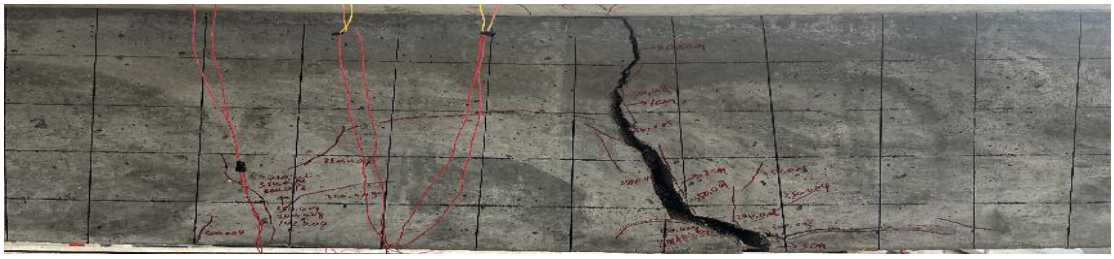

(c)

Fig. 6 - Failure pattern of test specimens: (a) RC-TH0; (b) UN-TH30; (c) UN-TH50

Load-Deflection Relationship

As shown in Figure 7(a), the load-deflection curves of the T-beams initially display a linear trend, indicating behavior within the elastic phase. As the applied load increases, the slope of the curves decreases, marking the transition into the elastic-plastic phase, characterized by a gradual reduction in stiffness. As the T-beams approach peak load, their mechanical responses begin to diverge; for RC-TH0, the load remains relatively stable while displacement increases significantly, indicating the yielding stage and the onset of ductile damage. In contrast, the loads for UN-TH30 and UN-TH50 drop rapidly after peaking. This behavior is attributed to the propagation of the primary crack in the UHPC, with the remaining NC working in conjunction with the steel reinforcements. These observations align with the observed failure modes. Figure 7(b) presents the relative slip at the NC-UHPC interface, showing that the slip for UN-TH50 is significantly smaller than that of UN-TH30 upon reaching peak load. This difference can be explained by the increased thickness of the UHPC layer, which enhances stiffness, delays structural deformation, and suppresses the progression of interfacial slip.

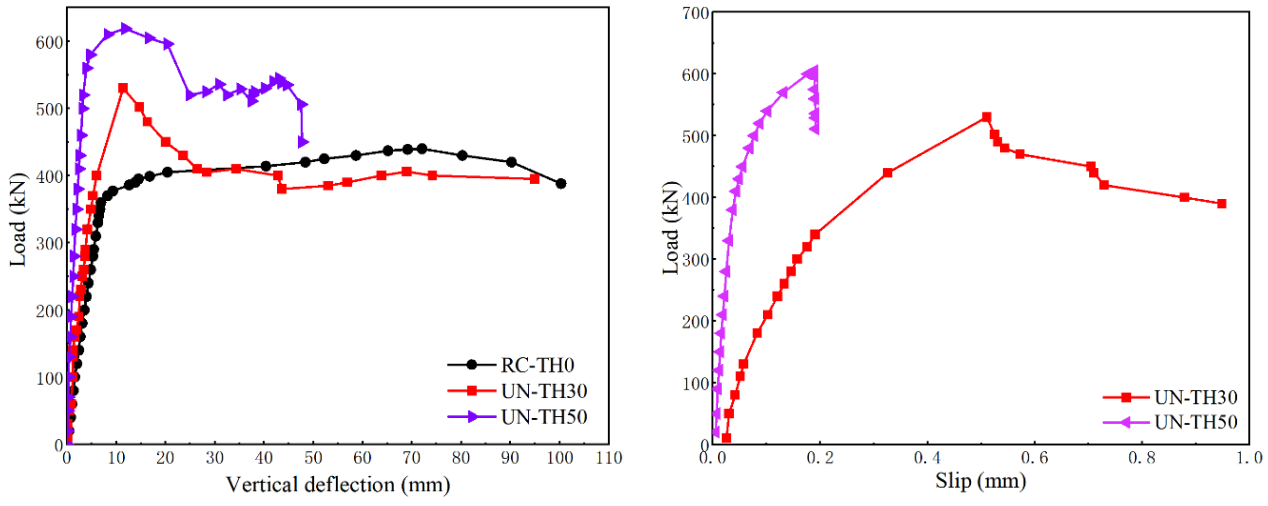

(a) *(b)*

Fig. 7 - Deflection and interface slips: (a) Load-deflection curve; (b) Load-interface slip curve

Table 2 presents the load characteristics of the tested T-beams, where P_c represents the cracking load, P_y denotes the yield load, δ_y corresponds to the deflection at yield; P_u refers to the ultimate load, δ_u corresponds to the deflection at the ultimate load; and K is the ratio of the yield load to the corresponding deflection, which reflects the bending stiffness of the beam.

Tab. 2 - Summary of test results

Specimen code	P_c (KN)	P_y (kN)	P_u (kN)	δ_y (mm)	δ_u (mm)	K (kN/mm)
RC-TH0	60.4	360.2	440	6.91	72.05	52.12
UN-TH30	102.7	402.1	530.4	6.01	11.39	66.91
UN-TH50	205.9	561.3	619.3	4.02	11.80	139.62

Figure 8 presents the load characteristic values for each test specimen. The data indicate that incorporating UHPC at the bottom of the T-beam significantly enhances its structural performance, positively influencing the cracking, yielding, and ultimate load. Specifically, the most considerable improvement is observed in the cracking load, which can increase by as much as 241%. As the thickness of the UHPC is increased from 0 mm to 30 mm and subsequently to 50 mm, the yielding load of the beam demonstrates increments of 11.6% and 55.8%, respectively. Correspondingly, the ultimate load exhibits increases of 20.5% and 40.8%, respectively. These findings clearly illustrate that the reinforced UHPC layer effectively enhances T-beams' flexural performance.

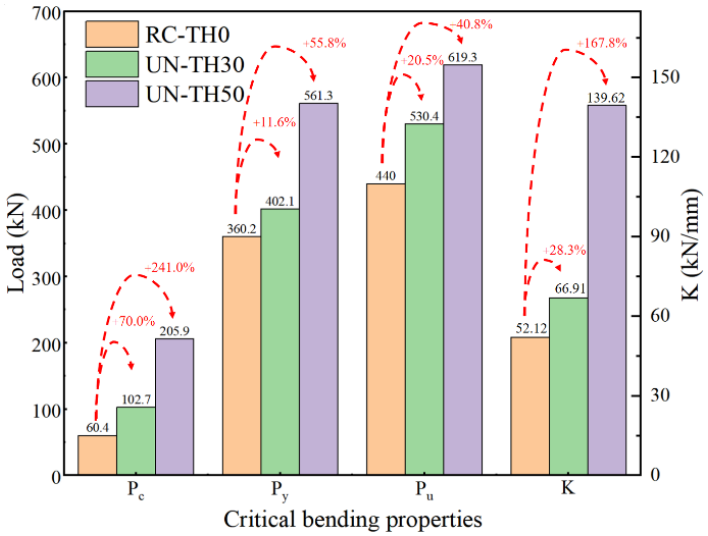

Fig. 8 - Critical mechanical properties

Strain History

Figure 9 illustrates the strain history of T-beams' mid-span reinforced with UHPC. The strain distribution along the height of the T-beam is linear as the load increases, indicating that the mid-span section adheres to the plane section assumption. The strain profiles demonstrate a clear linear relationship between strain and height at various load stages. At lower loads (e.g., $0.1P_u$), compressive strains dominate near the top of the beam, transitioning linearly to tensile strains toward the bottom. As the load increases to $0.9P_u$, the strain gradient becomes more pronounced, with maximum tensile strains exceeding 1,000 με at the bottom of the T-beam, while compressive strains near the top approach -200 με. It is observed that the neutral axis shifts slightly upward with higher loads, reflecting the gradual engagement of UHPC's tensile capacity. Both UHPC-reinforced T-beams exhibit minimal deviation from linearity, even near peak loads, underscoring the effectiveness of UHPC in maintaining sectional compatibility, which is crucial for accurately predicting the flexural behavior of strengthened T-beams under both service and ultimate loads.

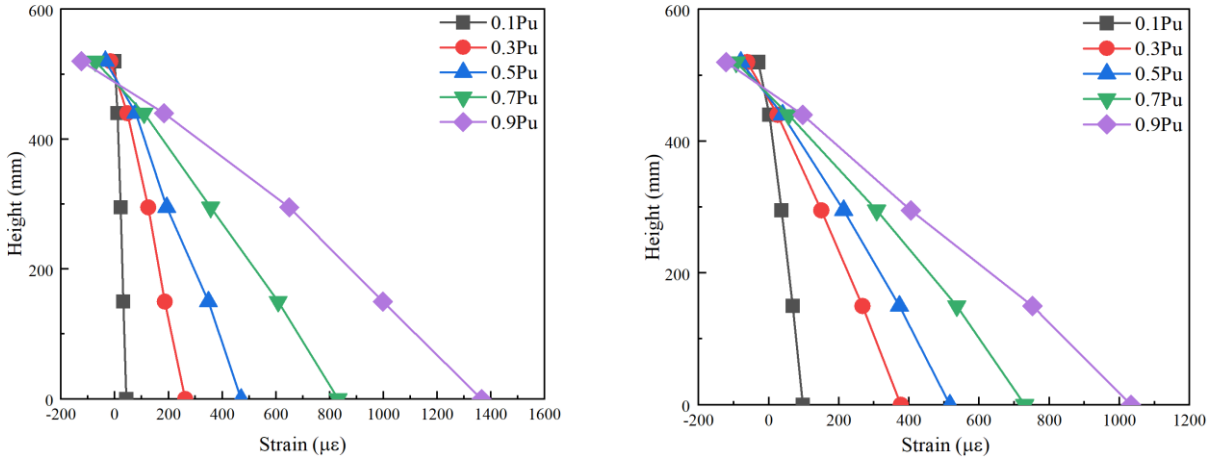

Fig. 9 - Strain distribution at mid-span section: (a) UN-TH30; (b) UN-TH50

Verification of Computational Model

Verification using Current Experimental Results

Table 3 compares the theoretical and experimental bending capacities of UHPC-reinforced T-beams. For ultimate loads, the experimental results exceed theoretical predictions by 6.3 to 9.5%, with all relative errors remaining below 10%, demonstrating the conservative reliability of the proposed model. This systematic underestimation in calculations ensures a built-in safety margin, validating the model's applicability for practical design while prioritizing structural safety under ultimate load conditions. For cracking loads, the errors between the experimental data and the theoretically calculated results range from 5.0% to 9.3%. However, the theoretical cracking load for beam UN-TH30 is higher than the experimental value, which may indicate insufficient reliability of the computational model. The underlying reason could be that significant residual tensile stresses existed in the original beam. These residual stresses, upon superposition with the stresses induced by the subsequently applied loads, resulted in higher actual tensile stresses in the UHPC layer. Furthermore, the prolonged storage time of the original beam may have led to a reduction in the elastic modulus of the concrete, while the UHPC retained a relatively high elastic modulus. The increased stiffness discrepancy between the two materials worsened deformation compatibility, generating additional bending stresses at the interface and accelerating crack initiation in the UHPC layer. Consequently, the experimentally measured cracking load of beam UN-TH30 was lower than predicted.

Tab. 3 - Comparison between theoretical and experimental values

	Specimen code	Theoretical value (kN)	Experimental value (kN)	Relative error (%)
Ultimate loads	RC-TH0	402.4	440.0	8.5
	UN-TH30	497.2	530.4	6.3
	UN-TH50	560.5	619.3	9.5
Cracking loads	RC-TH0	56.7	60.4	6.1
	UN-TH30	112.3	102.7	-9.3
	UN-TH50	195.6	205.9	5.0

Verification using Experimental Data in Literature

To further validate the accuracy of the computational model for predicting the flexural capacity of reinforced concrete T-beams strengthened with a thin UHPC layer, experimental data from twenty-seven groups of flexural tests on UHPC-strengthened T-beams in Reference [17-20] were selected for comparison. The comparison between the calculated ultimate flexural capacities and the experimental results is presented in Figure 10. As shown in Figure 10, the computational model accurately predicted the ultimate flexural capacity of UHPC-strengthened T-beams. The errors between the theoretical and experimental valus are all within 10%, with the theoretical values are generally slightly lower than the experimental values. This indicates that the computational model not only provides precise predictions but also maintains a certain safety margin, which holds significant practical value for engineering applications.

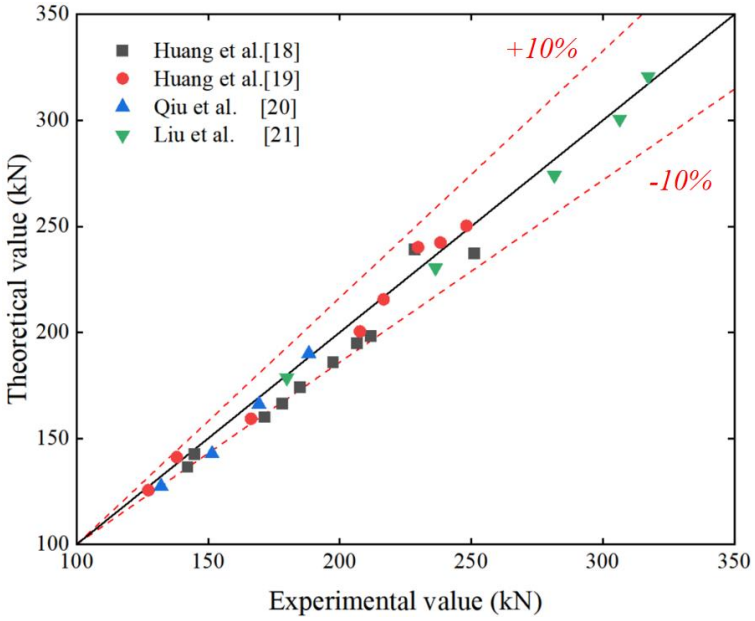

Fig. 10 - Comparison of theoretical and experimental values

CONCLUSION

This study systematically examined the flexural behavior of UHPC-reinforced T-beams through experimental testing and theoretical modeling. Three specimens with UHPC layers of varying thicknesses (0 mm, 30 mm, and 50 mm) were fabricated and subjected to four-point bending until failure. The failure mechanisms, load-displacement characteristics, and strain evolution were analyzed. A predictive model for flexural capacity was developed using the converted section method, integrating experimental observations with code-based principles. Key findings are summarized as follows:

(1) UHPC layer significantly changes the failure mode of T-beams while enhancing their flexural performance. T-beams with 30 mm and 50 mm UHPC layers demonstrated 28.3% and 167.8% increases in flexural stiffness, respectively, compared to the unreinforced beam. Corresponding improvements in ultimate resistance reached 20.5% and 40.8%, highlighting the efficacy of UHPC in structural strengthening.

(2) Strain distributions across the T-beam height under bending moment adhered closely to the flat section assumption. Linear strain gradients were consistently observed throughout the loading process, validating the applicability of classical beam theory to UHPC-reinforced systems.

(3) The proposed predictive model, based on the converted section method, demonstrated conservative yet reliable estimates of flexural capacity. Experimental results exceeded theoretical predictions by up to 9.5%, confirming the model's inherent safety margin. This discrepancy underscores the model's suitability for engineering design applications, ensuring robustness while accounting for material and geometric uncertainties.

(4) The existing methodology exclusively evaluates alterations in flexural bearing capacity subsequent to the application of UHPC thin-layer reinforcement, neglecting to consider additional factors such as potential degradation that may occur over extended periods of use. Future research efforts are needed to emphasize the investigation of the long-term performance characteristics of steel beams.

ACKNOWLEDGMENTS

The authors express their sincere gratitude for the financial support provided by the Science and Technology Project of Guangzhou (Grant # 2024A04J9888), the National Natural Science Foundation of China (Grant # 52278161), and the Guangdong Basic and Applied Basic Research Foundation (Grant # 2023A1515010535).

REFERENCE

[1] Chen, M., 2013. The application of structural adhesives in the bridge reinforcement. Advanced Materials Research, 655, p.2288-2293. Doi: org/10.4028/www.scientific.net/AMR.655-657.2288

[2] He, S. H., Zhou, D. F., Bai, B. S., et al. 2025. Experimental Study on Shear Performance of Prefabricated HSS-UHPC Composite Beam with Perfobond Strip Connectors. Engineering Structures, 324: 119318. Doi: org/10.1016/j.engstruct.2024.119318

[3] Ismail, M.K. Hassan, A.A., 2021. Structural performance of large-scale concrete beams reinforced with cementitious composite containing different fibers. Structures, 31, p.1207-1215. Doi: org/10.1016/j.istruc.2021.02.028

[4] Gong, Y. F., 2022. Application research of external prestressing technology in bridge reinforcement construction. TranspoWorld, 07, p.18-19. Doi: 10.16248/j.cnki.11-3723/u.2022.07.003

[5] Wang, S. H., Liao, J. S., et al. 2025. Analysis of maintenance and reinforcement techniques for dangerous old bridges and their application effects. Western China Communications Science & Technology, 05, p.156-158. Doi: 10.13282/j.cnki.wccst.2025.05.046

[6] Wu, W, 2024. Analysis on the design method of highway bridge structure reinforcement. Constructions & Design for Project, 22, p.58-60. Doi: org/10.13616/j.cnki.gcjsysj.2024.11.218

[7] He, S. H., Zhong, H. Q., Huang, X., et al. Experimental Investigation on Shear Fatigue Behavior of Perfobond Strip Connectors Made of High Strength Steel and Ultra-High Performance Concrete. Engineering Structures, 2025, 322(B): 119181. Doi: org/10.1016/j.engstruct.2024.119181

[8] Brühwiler, E., Denarié, E., 2013. Rehabilitation and strengthening of concrete structures using ultra-high performance fibre reinforced concrete. Structural Engineering International, 23(4), p.450-457. Doi: org/10.2749/101686613X13627347100437

[9] Tazarv, M., Saiidi, M. S., 2015. UHPC-filled duct connections for accelerated bridge construction of RC columns in high seismic zones. Engineering Structures, 99, p.413-422. Doi: org/10.1016/j.engstruct.2015.05.018

[10] Wang, S. L., 2017. Construction technology of through inclined steel box arch ribs for Yunzaobang Bridge. Traffic Engineering and Technology for National, 01, p.57-60. Doi: org/10.13219/j.gjgyat.2017.01.015

[11] Yin, H., Teo, W., Shirai, K., 2017. Experimental investigation on the behaviour of reinforced concrete slabs strengthened with ultra-high performance concrete. Construction and Building Materials, 155: p.463-474. Doi: org/10.1016/j.conbuildmat.2017.08.077

[12] Men, P. F., Di, J., Qin, F. J., et al., 2024. Bending behaviour of reinforced concrete T-beams damaged by overheight vehicle impact strengthened with ultra-high performance concrete (UHPC) . Case Studies in Construction Materials, 21, e03393. Doi: org/10.1016/j.cscm.2024.e03393

[13] Ministry of Transport of the People's Republic of China, 2008. Specifications for strengthening design of highway bridges: JTG/T J22—2008. People's Communications Press. http://www.csres.com/detail/193999.html

[14] Yang, K. H., 2019. Axial behavior of reinforced concrete columns strengthened with new section enlargement approaches. ACI Structural Journal, 166(5), p.87-96. Doi: org/10.14359/51715631

[15] Ministry of Housing and Urban-Rural Development of the People's Republic of China, 2019. Standard for test methods of concrete physical and mechanical properties: GB/T 50081-2019. China Architecture Building Press. http://www.csres.com/detail/333787.html

[16] AQSIQ and SAC(General Administration of Quality Supervision, Inspection and Quarantine of the People's Republic of China and Standardization Administration of the People's Republic of China). Reactive Powder Concrete: GB/T 31387-2015. Standards Press of China, 2015. http://www.csres.com/detail/259316.html

[17] Huang, Z. P., et al. 2023. Flexural behaviour of concrete T-beams damaged by overheight vehicle impact reinforced with UHPC. Case Studies in Construction Materials, 21. Doi: 10.1016/j.cscm.2024.e03393

[18] Huang, S., et al. 2024. Flexural behaviour of damaged concrete T-beams reinforced with ultra-high performance concrete filling. Frontiers in Materials, 11. Doi: 10.3389/fmats.2024.1410016

[19] Qiu, M. H., et al. 2020. Experimental investigation on flexural behavior of reinforced ultra high performance concrete low-profile T-beams. International Journal of Concrete Structures and Materials, 14. Doi: 10.1186/s40069-019-0380-x

[20] Liu, C., et al. 2019. Calculation method for flexural capacity of high strain-hardening ultra-high performance concrete T-beams. Structural Concrete, 20, p.405-419. Doi: 10.1002/suco.201800151